Supplementary Information (SI) for Journal of Materials Chemistry A.
This journal is © The Royal Society of Chemistry 2026

Supplementary Information

First-Principles Study of Dual-Site Sr–M (M = Ga, Hf, Ge) Co-Doping in the Perovskite Solid Electrolyte $Li_{0.5}La_{0.5}TiO_3$: Effects on Li^+ Migration and Electronic Insulation

"Arifur Rahman[a], Sheraz Ahmad[b], Oueslati Abderrazek[c], Zhen Zhou[d,e], Nouari Saheb[a,b*]

[a] Department of Mechanical Engineering, King Fahd University of Petroleum and Minerals, Dhahran, 31261, Saudi Arabia
[b] Interdisciplinary Research Centre for Advanced Materials, King Fahd University of Petroleum and Minerals, Dhahran, 31262, Saudi Arabia
[c] Laboratory of Spectroscopic Characterization and Optics of Materials, Faculty of Sciences, University of Sfax, Tunisia
[d] School of Energy Science and Technology, Henan University, Zhengzhou 450046, Henan, China
[e] Collaborative Innovation Center of Materials Science, Nankai University, Tianjin 300350, P.R. China

Corresponding Author: Nouari Saheb nouari@kfupm.edu.sa"

Lattice optimization

Table S1. Lattice constant optimization of $Li_{0.5}La_{0.5}TiO_3$ (LLTO)

Li0.5La0.5TiO3 (LLTO)		
Lattice constant (Å)		Energy (eV)
a=b	c	
3.86	7.8	-82.01491266
3.87	7.8	-82.03197054
3.88	7.8	-82.04402765
3.89	7.8	-82.05113234
3.9	**7.8**	**-82.05487884**
3.91	7.8	-82.05487535
3.92	7.8	-82.05029408
3.93	7.8	-82.04108716
3.94	7.8	-82.02886016
3.95	7.8	-82.01104213

Table S2 Wyckoff sites, fractional atomic coordinates, and occupancies of LLTO

Atom	Wyckoff	x	y	z	Occ
La	1a	0.00000	0.00000	0.00000	0.5
Li	1a	0.00000	0.00000	0.00000	0.5
La	1b	0.00000	0.00000	0.50000	0.5
Li	1b	0.00000	0.00000	0.50000	0.5
Ti	2h	0.50000	0.50000	0.263	1.0
O	1c	0.50000	0.50000	0.00000	1.0
O	1d	0.50000	0.50000	0.50000	1.0
O	4i	0.00000	0.50000	0.240	1.0

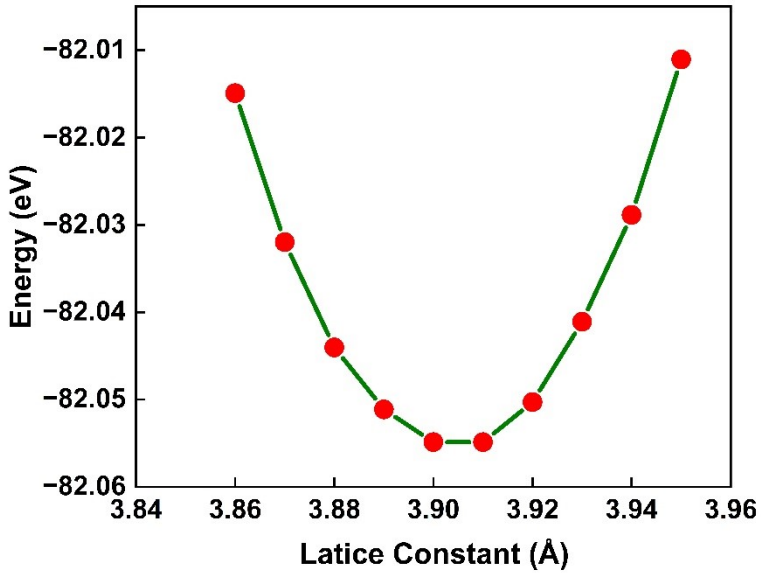

Fig. S1. Lattice constant optimizations of pristine LLTO unitcell.

Table S3 Calculated thermodynamic stability metrics for Sr–Ga, Sr–Hf, and Sr–Ge co-doped LLTO systems.

System	E_hull (eV atom^{-1})	Δμ_O stability window (O rich and O poor) (eV)
Sr–Ga LLTO	0.109	−11.40 to −4.94
Sr–Hf LLTO	0.121	−11.40 to −4.94
Sr–Ge LLTO	0.072	−11.54 to −4.94

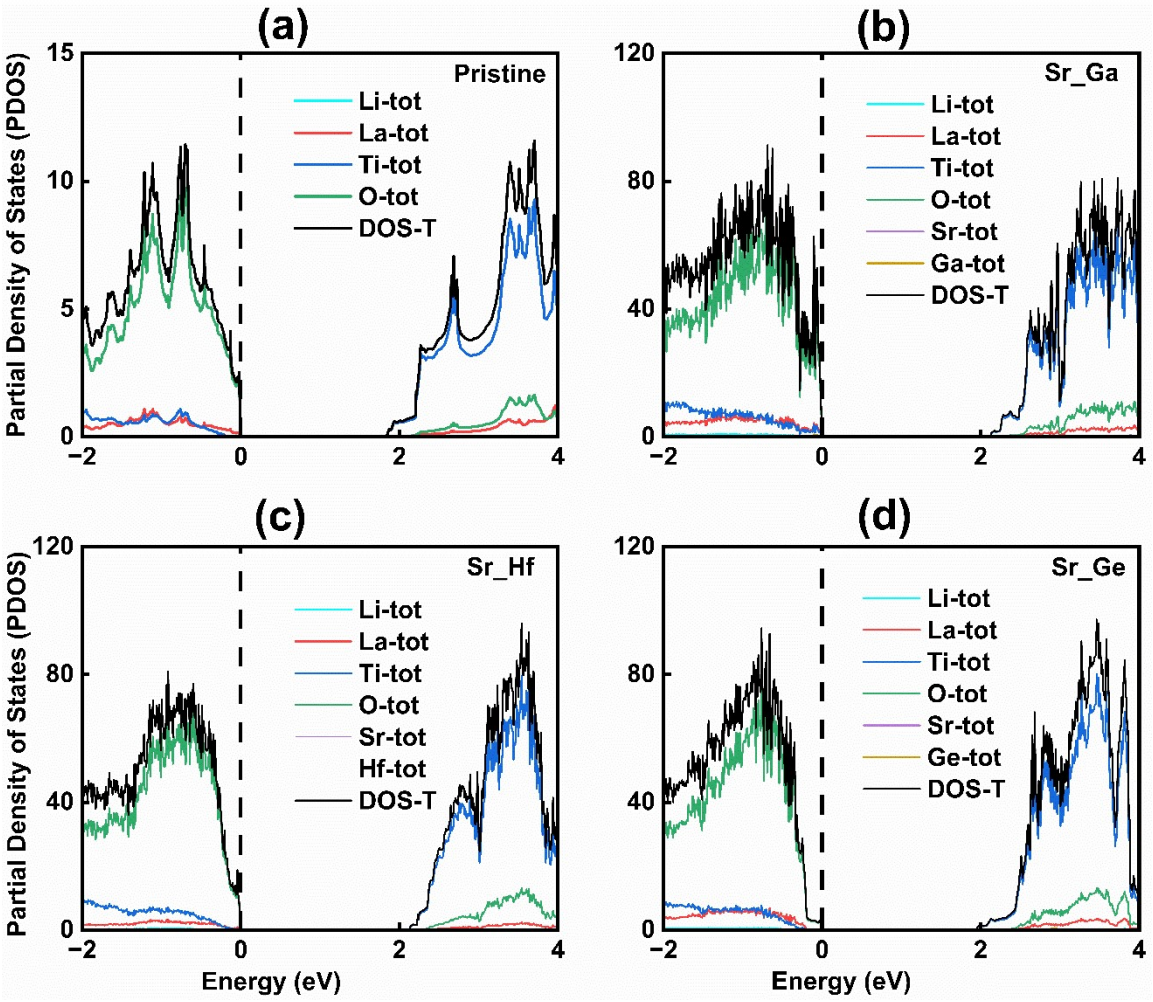

Fig. S2. Panels (e–h) show the total density of states (TDOS) and projected density of states (PDOS) for (e) pristine, (f) Sr–Ga co-doped, (g) Sr–Hf co-doped, and (h) Sr–Ge co-doped LLTO. The Fermi level is set to 0 eV (dashed line). The band gap values are indicated in each band structure plot.

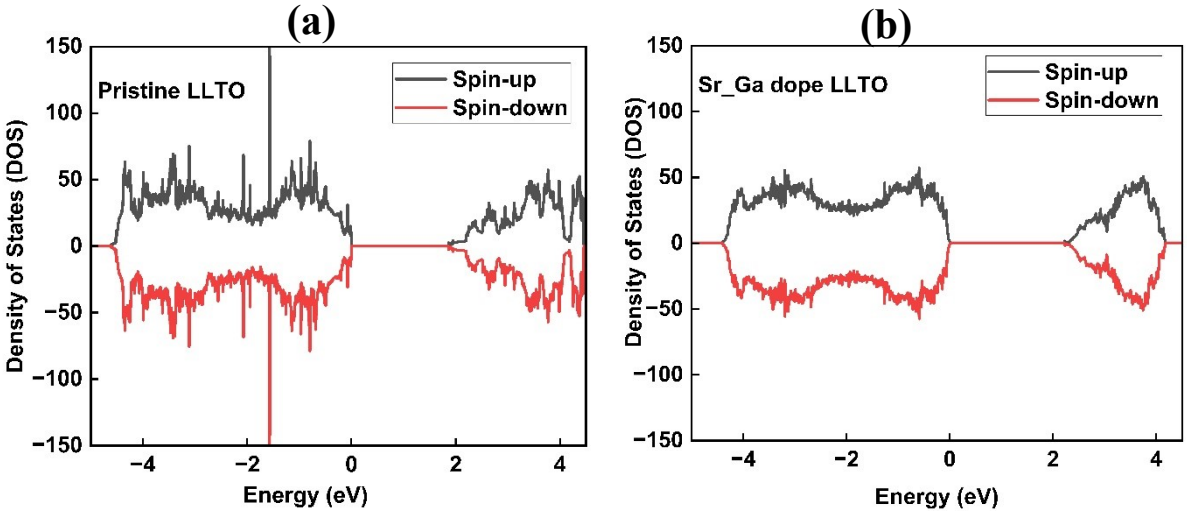

Fig. S3. Spin polarized density of states of (a) pristine (b) Sr-Ga dope LLTO.

Atomic structures obtained from ab initio molecular dynamics (AIMD) simulations for pristine and Sr–Ga, Sr–Hf, and Sr–Ge co-doped LLTO at 800 K upto 20 ps.

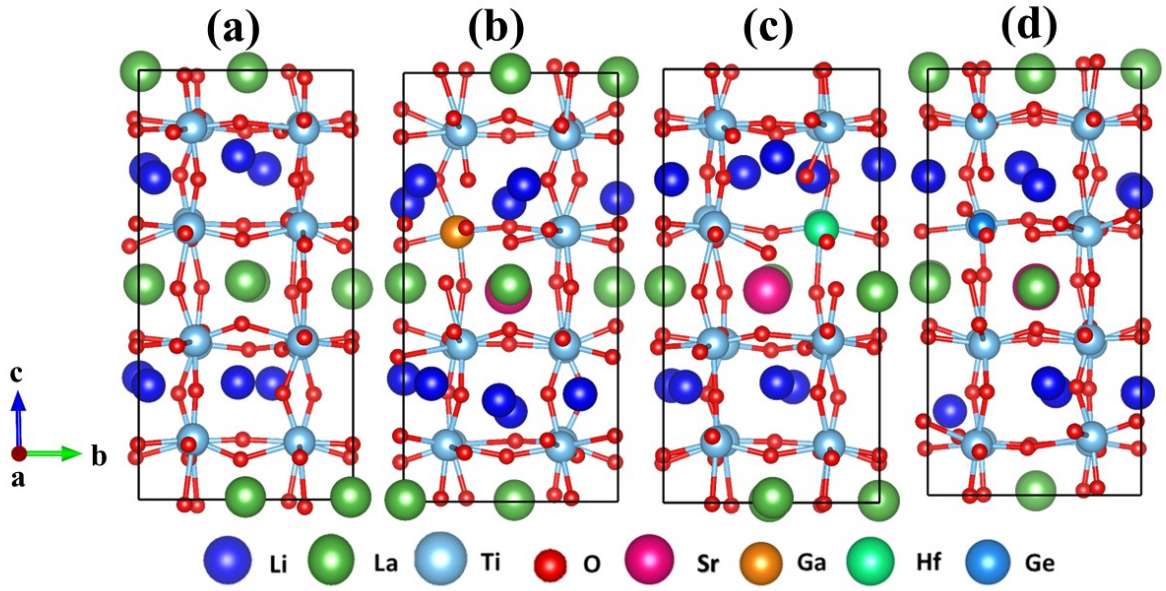

Fig. S4. Atomic structures of (a) pristine LLTO, (b) Sr–Ga co-doped LLTO, (c) Sr–Hf co-doped LLTO, and (d) Sr–Ge co-doped LLTO during AIMD simulations at 800 K for up to 20 ps.

To maintain a charge-neutral, ionically compensated model using only Li

The defect model described here corresponds to the same charge-compensated supercell ($Li_{10}La_7SrTi_{15}MO_{48}$; M = Ga, Hf, Ge) used in the main manuscript. A 2 × 2 × 2 LLTO supercell ($La_8Li_8Ti_{16}O_{48}$, 80 atoms) was adopted as the pristine reference. Aliovalent co-doping was introduced by substituting one La atom with Sr and one Ti atom with M, accompanied by the removal of one Li atom to create a Li vacancy. Within the formal oxidation-state framework (La^{3+}, Ti^{4+}, O^{2-}, Li^{+}), the combined defect set (V_Li + Sr_La + M_Ti) results in a net −3 charge imbalance relative to the pristine system. To maintain charge neutrality in the DFT supercell, three additional Li atoms were introduced as compensating species. These compensating Li atoms were initially placed at candidate fourfold oxygen-coordinated window/interstitial sites, consistent with experimental evidence that Li preferentially occupies such positions in LLTO rather than the larger A-site cavities [1].

Because aliovalent substitution breaks local symmetry and introduces multiple inequivalent Li configurations, ten distinct initial arrangements of the compensating Li atoms were generated and fully relaxed under identical computational conditions. The lowest-energy configuration was selected as the representative defect structure for subsequent analysis. The resulting charge-neutral supercell corresponds to the composition $Li_{10}La_7SrTi_{15}MO_{48}$, which can be normalized to $Li_{1.25}La_{0.875}Sr_{0.125}Ti_{1.875}M_{0.125}O_6$.

Defect formation energies were evaluated using the standard chemical-potential formalism, where the formation energy is defined by the total energy difference between defective and pristine supercells, together with the exchange of atoms with external reservoirs [23].

Table S4. minimum energy position for 3-Li placements

Position	Energy
1	-486.86468042
2	**-487.11242300**
3	-486.81004112
4	-486.93098926
5	-486.39961401
6	**-487.19795277**
7	**-487.05949282**
8	-486.99754018
9	-487.03731037
10	-486.72490443

Diffusion Barrier Energy

To quantify the kinetic feasibility of Li-ion transport in LLTO, the Li-ion diffusion barrier energy (migration barrier, E_m) was evaluated using the nudged elastic band (NEB) method as implemented in VASP. In NEB, Li migration is treated as a hopping event between two locally stable sites, and a series of intermediate "images" are generated between the fully relaxed initial and final states; these images are then relaxed to determine the minimum-energy path (MEP) and its saddle point, with the barrier defined as the maximum energy along the MEP relative to the initial state. Consistent with a vacancy-mediated mechanism, NEB endpoints were constructed from fully relaxed structures corresponding to a nearest-neighbor Li–vacancy exchange, and the migration barrier was obtained using climbing-image NEB to accurately locate the transition state. A suitable supercell was constructed to ensure that the migration pathway was fully contained within the interior of the crystal, thereby minimizing interactions between periodic images. Specifically, for VLi-LLTO, a $3 \times 2 \times 1$ supercell was employed to model Li migration along the a- and b-directions, ensuring adequate separation of the vacancy and diffusion pathway within the periodic framework.

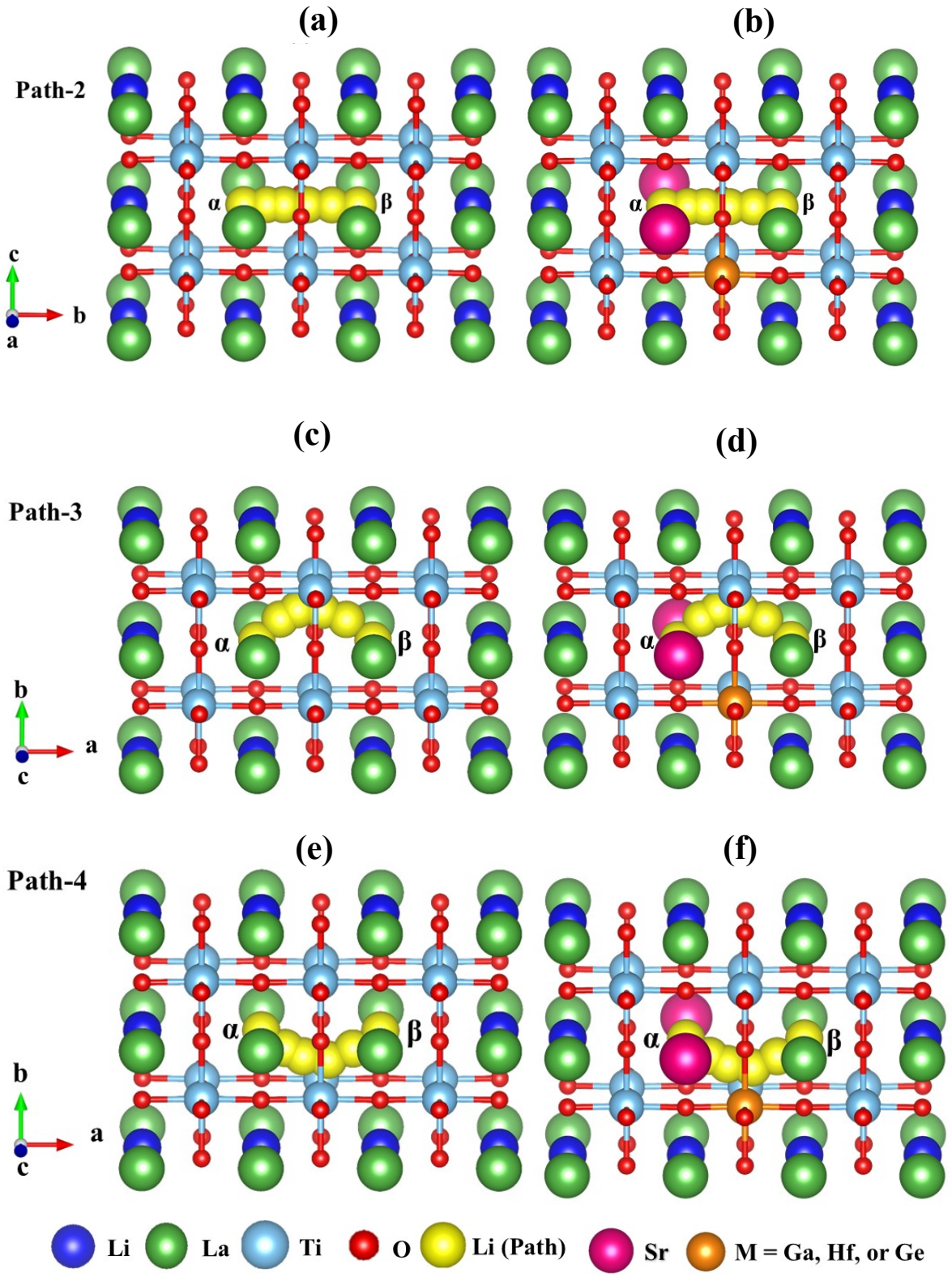

Figure S5 The nudged elastic band (NEB) calculates images of Li^+ diffusion path-2,3,4 along along b axis for (a) pristine (b) dope, and a-axis curve path (up) (c) pristine, (d) dope, along a-axis curve path (down) of (e) pristine, (f) dope 3×2×1 and 2×3×1 $Li_{0.5}La_{0.5}TiO_3$ (LLTO) supercell respectively.

References

1 J. A. Alonso, J. Ibarra, M. A. Paris, J. Sanz, J. Santamaria, C. LeÓn, A. Vdrez and M. T. Fermandez, MRS Proceedings, 1999, 575, 337–342.

2 B. S. Youmbi, S. Zékeng, S. Domngang, F. Calvayrac and A. Bulou, Ionics (Kiel)., 2012, 18, 371–377.

3 S. B. Zhang and J. E. Northrup, Phys. Rev. Lett., 1991, 67, 2339.